

Investigation of Kelvin probe force microscopy efficiency for the detection of hydrogen ingress by cathodic charging in an aluminium alloy

Céline Larignon,^a Joël Alexis,^b Eric Andrieu,^a Loïc Lacroix,^b Grégory Odemer^a and Christine Blanc^{a,*}

^aUniversité de Toulouse, CIRIMAT, UPS/INPT/CNRS, ENSIACET, 4 allée Emile Monso, BP 44362, 31030 Toulouse Cedex 4, France

^bUniversité de Toulouse, LGP, ENIT, 47 avenue d'Azereix, BP 1629, 65016 Tarbes Cedex, France

Received 5 October 2012; revised 22 November 2012; accepted 23 November 2012

Available online 3 December 2012

Detecting and locating absorbed hydrogen in aluminium alloys is necessary for evaluating the contribution of hydrogen embrittlement to the degradation of the mechanical properties for corroded or cathodically hydrogen-charged samples. The capability of Kelvin probe force microscopy (KFM) to overcome this issue was demonstrated. Aluminium alloy samples were hydrogenated by cathodic polarization in molten salts ($\text{KHSO}_4/\text{NaHSO}_4\text{-H}_2\text{O}$). The presence of absorbed hydrogen was revealed; the affected zone depth was measured by secondary ion mass spectroscopy analyses and KFM measurements.

© 2012 Acta Materialia Inc. Published by Elsevier Ltd. All rights reserved.

Keywords: Kelvin probe force microscopy (KFM); Secondary ion mass spectroscopy (SIMS); Hydrogen diffusion; Aluminum alloys

Kelvin probe force microscopy (KFM) is a powerful tool for studying the local surface potential. It allows, via an atomic force microscopy (AFM)-associated mode, the mapping of both the topography of any material surface in air with high spatial resolution and the corresponding surface potential (or so-called contact potential difference). KFM is based on the vibrating capacitor method (Kelvin method) [1] adapted to an AFM probe. Since its first use for measuring the contact potential difference at the nanometer scale [2–4], this technique has been used to study electrochemical mechanisms [5] and localized corrosion [6–9]. Masuda [10] studied the stress corrosion cracking (SCC) of SUS304 stainless steel by KFM and attributed the surface potential variations to hydrogen produced by cathodic reactions. However, the use of KFM to detect hydrogen in metals and alloys has not yet been proved. Moreover, hydrogen embrittlement (HE) is suspected to play a major role in the SCC of aluminium alloys [11], the correlation between HE and SCC having been shown for other metals [12]. It was therefore important to develop a method to identify hydrogen traps in alu-

minium alloys. Secondary ion mass spectroscopy (SIMS) does not readily distinguish corrosion products from atomic hydrogen, and its spatial resolution can be limited. In this context, the aim of this paper is to evaluate for the first time the possibility of detecting and quantifying absorbed hydrogen in an AA 2024 aluminium alloy by KFM. To this end, we chose to study cathodically hydrogen-charged samples to ensure that enough hydrogen was present in the material. We performed SIMS analyses on the samples and compared the SIMS results with those obtained using KFM to evaluate the efficiency of KFM.

The material studied in the present work was a 2024 T351 aluminium alloy rolled plate (50 mm thick) with the composition (in wt.%): 4.46% Cu, 1.44% Mg, 0.60% Mn and 0.13% Fe [13]. Its microstructure was presented in a previous work [13]; it is composed of grains elongated along the rolling direction (RD), with average grain dimensions in the rolling, long transverse (LT) and short transverse (ST) directions, of 700, 300 and 100 μm , respectively. Both intragranular precipitates, such as Al–Cu–Mn–Fe and Al_2CuMg particles, and intergranular precipitates (mainly Al_2CuMg and Al–Cu–Mn) can be observed, using an optical or scanning electron microscope and a transmission electron

* Corresponding author. Tel.: +33 5 34 32 34 07; fax: +33 5 34 32 34 98; e-mail: christine.blanc@ensiacet.fr

microscope, respectively. No precipitate-free zone was observed along the grain boundaries in the as-received plate. To allow for KFM and SIMS analyses after hydrogen charging without any further surface preparation, the sample dimensions were $2 \times 3 \times 3 \text{ mm}^3$ (LT \times ST \times RD). The samples were H-charged in the ST/LT side and analysed in the ST/RD side. Thus, the ST/LT and ST/RD sides were mechanically polished down to 3 and 0.25 microns, respectively, using SiC paper and diamond paste with distilled water as a lubricant. The samples were ultrasonically cleaned in ethanol and dried in air.

Hydrogen was introduced into the alloy by cathodic charging in a molten salt of 53.5 wt.% KHSO_4 and 46.5 wt.% $\text{NaHSO}_4 \cdot \text{H}_2\text{O}$ at 150°C with an applied potential of -1 V vs. Ag/Ag^+ . To ensure hydrogen penetration from the ST/LT side only, samples were embedded in epoxy resin with a 6 mm^2 area on the ST/LT side exposed to the electrolyte. Three different charging durations were tested: 7, 24 and 72 h. The charging temperature was low enough that it did not modify the microstructure of the AA 2024-T351 by artificial ageing. However, the temperature was also high enough to ensure efficient hydrogen penetration for a reasonable charging duration. Furthermore, the charging durations were chosen to correspond to a sufficient hydrogen penetration (several tens of microns) for study by local techniques, such as SIMS and KFM. After charging, the samples were removed from the epoxy resin and stored in liquid nitrogen to prevent hydrogen desorption.

The hydrogen contained in the samples was globally quantified using a Horiba EMGA-621W Instrumental Gas Analyser. The experimental method consists of melting the sample (0.2 g) by heating it to approximately 950°C and analysing the gases by thermal conductivity. The detection limit is approximately 1 ppm weight. To obtain profiles of hydrogen penetration, the local chemical composition of the H-charged samples was first analysed by SIMS using an IMS 4F/6F CAMECA analyser. A Cs^+ ion beam ($8 \mu\text{m}$ in diameter) was used. The hydrogen-to-aluminium signal ratio was used to overcome the aluminium signal variation from one grain to another. KFM measurements were then performed on a Nanoscope IIIa Multimode atomic force microscope from Digital Instruments equipped with a Quadrex electronic module. The probes were conductive Pt/Ir-coated silicon tips. The KFM potential scans were collected using the “lift” technique described in previous work [9], which allows the topography and potential to be obtained simultaneously, line by line, and with minimal cross-talk. This technique involves a two-pass rastering of the surface. During the first pass, the surface topography of a single line scan is acquired in standard tapping mode. Then, at a set lift height of 100 nm from the sample surface, the contact potential difference is recorded point-by-point using the Kelvin probe method [14]. All KFM measurements were performed in air at room temperature and in an ambient relative humidity of approximately 40%. The potential tip was verified as stable during each experiment; the KFM potential values are thus raw data without any post-treatment.

Open circuit potential (OCP) measurements were also performed on H-charged samples in 1 M NaCl using a

three-electrode conventional electrochemical cell, with the H-charged sample as the working electrode, a saturated calomel electrode as the reference and a platinum electrode as the counter electrode.

Preliminary diffusion calculations were performed to theoretically evaluate the maximum hydrogen penetration in the alloy using the second Fick’s law (transitory regime) for a semi-infinite system:

$$\frac{c(x) - c_S}{c_0 - c_S} = \text{erf}\left(\frac{x}{2\sqrt{Dt}}\right) \quad (1)$$

where D is the hydrogen diffusion coefficient (considered to be constant), t is the charging time, $c(x)$ is the hydrogen concentration at depth x , c_0 is the initial hydrogen concentration ($c_{0(t=0)} = 0$) and c_S is the surface hydrogen concentration ($c_{S(t=0)} = 1$). Two values for the hydrogen diffusion coefficient were chosen based on previously published results: $1 \times 10^{-7} \text{ cm}^2 \text{ s}^{-1}$ [15] and $2 \times 10^{-10} \text{ cm}^2 \text{ s}^{-1}$ [16]. Both values were proposed for pure aluminium and were used here although the microstructure of AA 2024 is more complex. As explained by Danielson [17], the large difference in diffusion coefficients is hypothesized to be due to the effect of aluminium oxide. The residual hydrogen concentration profiles showed that hydrogen charging durations are long enough for the hydrogenation penetration depth to be sufficient considering the spatial resolution for SIMS and KFM. Note that the calculations are based on approximations and do not account for hydrogen trapping. Thus, the effective hydrogen charging might differ from the theoretical results. To confirm the presence of hydrogen in the samples, the global hydrogen content of H-charged samples was evaluated by instrumental gas analysis, and the results were compared to those obtained for two non-charged AA 2024-T351 samples. For each charging duration, three samples were analysed. Whatever the charging duration, a non-negligible scattering of the hydrogen contents measured was observed, which could be attributed to the small sample size as well as a probable heterogeneous hydrogen distribution. Nonetheless, values between 4 and 6 ppm weight were obtained for the non-charged samples, corresponding to the residual hydrogen content in the alloy. Moreover, for the H-charged samples, the values measured were significantly higher than those of the non-charged samples, revealing that hydrogen had penetrated into the alloy. The results showed that, as expected, the hydrogen content increased when the charging duration increased, with mean values of 16, 22 and 27 ppm weight for 7, 24 and 72 h of charging, respectively.

In a second step, the diffusion profiles of hydrogen were plotted using SIMS on cathodically H-charged samples in the RD direction. The ratio between the hydrogen and aluminium signals (H/Al) was used to compensate for the aluminium signal variation from one grain to another. For all of the samples tested, a low H/Al signal was measured far from the H-charged side. The signal remained constant for a long distance, defining a baseline and confirming the presence of residual hydrogen in the material. For clarity, the residual hydrogen signal was subtracted from the values obtained and the corrected profiles of H/Al signals are presented in Figure 1. For the samples charged for 7 h, the

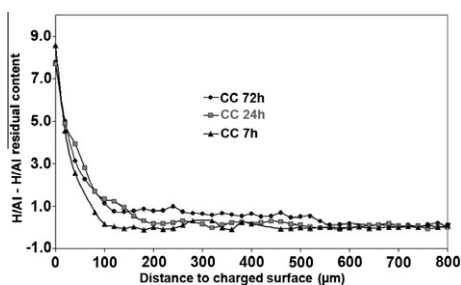


Figure 1. Normalized H/Al signal ratio (the H/Al signal for an H-charged sample was corrected by subtracting that for a non-charged sample) obtained by SIMS analyses for cathodically hydrogenated AA 2024-T351 samples at 150 °C in $\text{KHSO}_4/\text{NaHSO}_4 \cdot \text{H}_2\text{O}$ molten salts for 7, 24 and 72 h.

hydrogen content was significant near the surface and diminished rapidly away from it. For a distance from the H-charged side greater than $80 \pm 3 \mu\text{m}$, the H/Al signal stabilized at the reference value of the residual H/Al ratio. Therefore, the hydrogen penetration depth was estimated to be $80 \pm 3 \mu\text{m}$. For the samples charged for 24 h, the hydrogen penetration depth was approximately $300 \pm 3 \mu\text{m}$, whereas that for the samples charged for 72 h was $600 \pm 3 \mu\text{m}$. Based on the SIMS profiles, the apparent diffusion coefficients for 7, 24 and 72 h of charging were estimated to be 1×10^{-9} , 3×10^{-9} and $1.4 \times 10^{-8} \text{ cm}^2 \text{ s}^{-1}$, respectively. The error in the hydrogen penetration depth led to a negligible error in the diffusion coefficient. These values are in agreement with those from the literature for pure aluminium. A slight increase in the apparent coefficient with charging duration was observed, which supported the existence of trapping sites and/or microstructural short-circuits of diffusion. This variation of diffusion coefficients may also be related to the saturation of some specific traps. The longer the duration of the hydrogen charging, the stronger the H/Al signal, which was consistent with the interpretation of the SIMS analyses.

The study next focused on determining whether KFM was a relevant method of detecting hydrogen in aluminium alloys. Because the electrochemical potentials (OCPs) and KFM potentials have already been correlated by Stratmann et al. [18] and because OCP measurements are easy to perform, preliminary OCP measurements were carried out on H-charged samples. Considering that the hydrogen charging is performed in a molten salt bath at 150 °C and that the OCP can be modified by heat treatment, OCP measurements were also performed on H-free samples heat treated at 150 °C

for the same durations as for hydrogenation. These measurements allow the effect of the heat treatment to be distinguished from the effect of the hydrogen (Fig. 2(a)). The results first show that the OCP values decreased when the heat treatment duration time increased. Moreover, a comparison of the curves for the H-charged and heat-treated samples shows that the presence of hydrogen inside the aluminium alloy led to more cathodic OCP values. Therefore, OCP measurements appear to be sensitive to the presence of hydrogen considering that hydrogen could be responsible for the destabilization of the passive film; hence, an OCP profile as a function of the distance from the charged surface for H-charged samples was drawn in 1 M NaCl. Samples were cathodically charged for 72 h and then the OCP was measured at different depths using successive polishing (Fig. 2(b)). A polishing method was established so that the OCP values measured at different depths could be compared. The duration of the whole experiment was short; considering the low value of the hydrogen diffusion coefficient at room temperature, any possible hydrogen diffusion during the experiment was considered to be negligible. The profile shows that the OCP measured on the surface is much lower than that measured below the surface, which confirms the results shown in Figure 2(a). Moreover, the potential from a distance of approximately 430 microns stabilized around a value corresponding to the OCP of the 2024-T351 alloy heat treated for 72 h at 150 °C (Fig. 2(a)). Thus, the OCP measurements allowed the hydrogen diffusion depth to be estimated as $430 \pm 50 \mu\text{m}$. The apparent diffusion coefficient calculated from this method is $7 \pm 2 \times 10^{-9} \text{ cm}^2 \text{ s}^{-1}$.

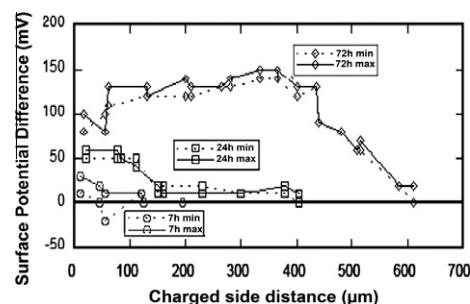


Figure 3. KFM potential difference profiles $\Delta V = V_\infty - V_x$ as a function of the H-charged side distance for H-charged AA 2024 samples for 7, 24 and 72 h in $\text{KHSO}_4/\text{NaHSO}_4 \cdot \text{H}_2\text{O}$ molten salts at 150 °C.

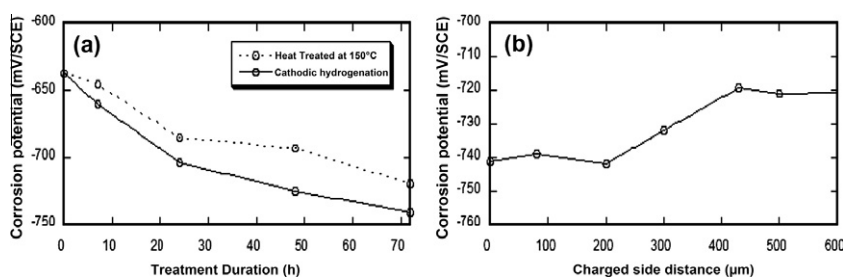


Figure 2. (a) Open circuit potential for AA 2024 H-charged samples and non-charged samples heat-treated at 150 °C as a function of the H-charging duration time in $\text{KHSO}_4/\text{NaHSO}_4 \cdot \text{H}_2\text{O}$ molten salts and/or the duration of the heat treatment at 150 °C. (b) OCP profile as a function of the distance from the H-charged side for a cathodically H-charged AA 2024 sample for 72 h. Electrolyte = 1 M NaCl.

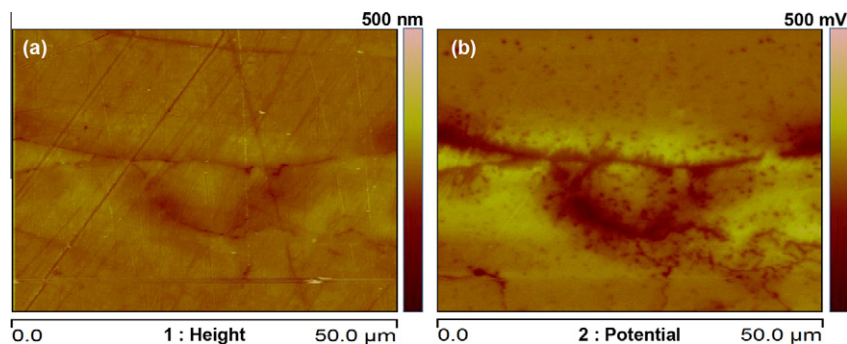


Figure 4. Topographical (a) and KFM potential (b) maps plotted around a corrosion defect grown on a 2024 T351 aluminium alloy during exposure to a 1 M NaCl solution.

The results show that OCP measurements were successfully applied to evaluate the hydrogen penetration depth, which suggested that KFM may be a relevant technique for such a study. KFM measurements were therefore performed using the same methodology as for SIMS analyses. To overcome the variation of the KFM potential of non-charged zone between samples, the difference $\Delta V = V_{\infty} - V_x$ between the potential far from the H-charged side, V_{∞} , and the potential at a given distance, V_x , was calculated. Figure 3 presents the ΔV profiles for all three hydrogenation duration times (7, 24 and 72 h). For each distance and hydrogenation time, four KFM measurements were performed on a line parallel to the H-charged side. Only two KFM potential values were reported: the minimum and maximum values. A positive potential difference reveals a KFM potential lower than that of the base material, i.e. far from the H-charged side. First, the KFM potential at the H-charged side is lower than that for the base metal potential, where hydrogen is absent. This result is in good agreement with previous OCP results. On the surface, the KFM potential difference is more important when the charging time is longer; this finding suggests that this potential difference is directly related to the local hydrogen content. Moreover, the longer the charging duration, the deeper the affected zone, with depth values for the H-enriched zone of 50 ± 10 , 400 ± 10 and 630 ± 10 μm for charging duration times of 7, 24 and 72 h, respectively. These values are in good agreement with those obtained using SIMS. Therefore, the apparent diffusion coefficients calculated with KFM are similar to those obtained by SIMS. A comparison of all of the results shows that the KFM potential differences are induced by the presence of hydrogen. Hence, it is possible to detect hydrogen in the AA 2024 using KFM measurements. The advantage of KFM is based on the possibility of working on the nanometric scale and therefore locating hydrogen very precisely, which is not possible using OCP measurements or SIMS analyses. Therefore, KFM measurements were performed on a 2024 aluminium alloy sample previously exposed to 1 M NaCl solution to develop intergranular corrosion defects. Figure 4 shows a topographical and a KFM potential maps plotted around a corrosion defect. The results showed that the KFM signal was different on and around the corrosion defect, which could be attributed to the presence of hydrogen in the corrosion defect and the diffusion of this element from the defect to the bulk. Further analysis of the application of

KFM measurements on corroded samples will be discussed in future work.

OCP measurements, KFM and SIMS analyses were combined to detect hydrogen in H-charged samples of a 2024 aluminium alloy. All three techniques allowed the hydrogen-affected depths and apparent hydrogen diffusion coefficients to be estimated as functions of the hydrogenation duration. The three techniques also produced almost identical results. Hence, the results presented here provide insight into the detection techniques for absorbed hydrogen, which is a key point for understanding material damage. KFM appears to be more flexible than SIMS, with the capability of exploring heterogeneities and absorbed hydrogen in aluminium alloys at the nanoscale. KFM is a cutting-edge technique for understanding corrosion damage-mechanical properties relationships for aluminium alloys.

- [1] Lord Kelvin, *Philos. Mag.* 46 (1898) 82.
- [2] Y. Martin, D.W. Abraham, H.K. Wickramasinghe, *Appl. Phys. Lett.* 52 (1988) 1103.
- [3] M. Nonnenmacher, M.P. O'Boyle, H.K. Wickramasinghe, *Appl. Phys. Lett.* 58 (1991) 2921.
- [4] J.M.R. Weaver, D.W. Abraham, *J. Vac. Sci. Technol. B9* (1991) 1559.
- [5] M. Böhmisch, F. Burmeister, A. Rettenberger, J. Zimmermann, J. Boneberg, P. Leiderer, *J. Phys. Chem. B* 101 (1997) 10162.
- [6] P. Schmutz, G.S. Frankel, *J. Electrochem. Soc.* 145 (1998) 2295.
- [7] V. Guillaumin, P. Schmutz, G.S. Frankel, *J. Electrochem. Soc.* 148 (2001) 163.
- [8] T.H. Muster, A.E. Hughes, *J. Electrochem. Soc.* 153 (2006) 474.
- [9] L. Lacroix, L. Ressler, C. Blanc, G. Mankowski, *J. Electrochem. Soc.* 155 (2008) 131.
- [10] H. Masuda, *Corros. Sci.* 49 (2007) 120.
- [11] H. Kamoutsi, G.N. Haidemenopoulos, V. Bontozoglou, S. Pantelakis, *Corros. Sci.* 48 (2006) 1209.
- [12] D. Delafosse, T. Magnin, *Eng. Fract. Mech.* 68 (2001) 693.
- [13] C. Larignon, J. Alexis, E. Andrieu, C. Blanc, G. Odemer, J.-C. Salabura, *J. Electrochem. Soc.* 158 (2011) 284.
- [14] H.O. Jacobs, H.F. Knapp, S. Muller, A. Stemmer, *Ultramicroscopy* 69 (1997) 39.
- [15] H. Saitoh, Y. Lijima, H. Takana, *Acta Metall. Mater.* 42 (1994) 2493.
- [16] G.A. Young, J.R. Scully, *Acta Mater.* 46 (1998) 6337.
- [17] M.J. Danielson, *Corros. Sci.* 44 (2002) 829.
- [18] M. Stratmann, H. Streckel, R. Feser, *Corros. Sci.* 32 (1991) 467.